Effect of Xe ion (167 MeV) irradiation on polycrystalline SiC implanted with Kr and Xe at room temperature

T. T. Hlatshwayo[1*], J. H. O'Connell[2], V. A. Skuratov[3], M. Msimanga[4], J. K. Kuhudzai[1], E. G. Njoroge[1], J. B. Malherbe[1]

[1] *Physics Department, University of Pretoria, Pretoria, South Africa*

[2] *Centre for HRTEM, Nelson Mandela Metropolitan University, Port Elizabeth, South Africa*

[3] *Joint Institute for Nuclear Research, Dubna, Russia*

[4] *Tshwane University of Technology, Department of Physics, P Bag X680, Pretoria 0001, South Africa*

*Corresponding author: thulani.hlatshwayo@up.ac.za

Abstract

The effect of swift heavy ion (Xe 167 MeV) irradiation on polycrystalline SiC individually implanted with 360 keV Kr and Xe ions at room temperature to fluences of 2×10^{16} cm^{-2} and 1×10^{16} cm^{-2} respectively, was investigated using transmission electron microscopy (TEM), Raman spectroscopy and Rutherford backscattering spectrometry (RBS). Implanted specimens were each irradiated with 167 MeV Xe^{+26} ions to a fluence of 8.3×10^{14} cm^{-2} at room temperature. It was observed that implantation of 360 keV Kr and Xe ions individually at room temperature amorphized the SiC from the surface up to a depth of 186 and 219 nm respectively. Swift heavy ion (SHI) irradiation reduced the amorphous layer by about 27 nm and 30 nm for the Kr and Xe samples respectively. Interestingly, the reduction in the amorphous layer was accompanied by the appearance of randomly oriented nanocrystals in the former amorphous layers after SHI irradiation in both samples. Previously, no similar nanocrystals were observed after SHI irradiations at electron stopping powers of 33 keV/nm and 20 keV/nm to fluences below 10^{14} cm^{-2}. Therefore, our results suggest a fluence threshold for the formation of nanocrystals in the initial amorphous SiC after SHI irradiation. Raman results also indicated some annealing of radiation damage after swift heavy ion irradiation and the subsequent formation of small SiC crystals in the amorphous layers. No diffusion of implanted Kr and Xe was observed after swift heavy ion irradiation.

K*eywords*: Swift heavy ion (SHI), implantation, Radiation damage, TEM, RBS, Raman spectroscopy

1. Introduction

Generation IV nuclear reactors, have a number of novel characteristics compared to the present generation nuclear reactors [1] such as higher efficiencies and increased safety. To increase the efficiency of these new reactors, they have to operate at high temperatures. This means that the moderator used cannot be light or heavy water but must be graphite. One of the key components to increase the safety of these reactors is non-leakage of radioactive fission products during accident conditions such as those at Fukushima. For this purpose the fuel elements in the new reactors employ multi-layered structures. The presently favoured fuel particles are the tri-structural-isotropic (TRISO) particles. In the TRISO particle, the kernel is coated by chemical vapour deposited SiC and pyrolytic carbon (PyC) layers [2]. One of the main characteristics of these coated fuel particles is their ability to retain fission products under all expected reactor conditions. In practice this means that the SiC and PyC layers must act as a diffusion barrier to radioactive fission products [2-6]. Usually radiation damage in SiC enhances or induces diffusion of some fission products.

In recent years our group at the University of Pretoria has been conducting research into several aspects of the TRISO coated fuel particles and in safe long-term storage of high-level radioactive waste. We have concentrated on aspects such as the diffusion of several fission products implanted in SiC, carbon, and the effects of vacuum annealing on radiation damage introduced by the relatively low energy implantation ions [2-12].

During the fission process in nuclear reactors, nuclides with a large range of energies are released, including energies in the order of 100 MeV i.e. the energy range of swift heavy ions (SHIs). SHIs lose most of their energy via electron excitations as they traverse a material until they have slowed down to the low energies where nuclear loss process dominates. It is well-known that a large amount of energy transferred into an electron subsystem of irradiated crystals may result, from a certain threshold value, in the formation of a specific radiation damage the so-called latent tracks [13]. Although not the only source of damage production, dense ionization may affect structure evolution by changing the charge state of defects or annealing due to intense local heating. Both the damage and the heat production in a nanometric volume surrounding the ion trajectory may affect the diffusion of the nuclides implanted in the substrate. Previously, only hundreds MeV heavy ion irradiation effects on electrically active dopant redistribution in silicon have been studied [14, 15].

Investigations on the creation of radiation damage in SiC by SHI irradiation and the annealing of radiation damage retained after implanting different low energy ions have been reported recently [16-23]. These studies seem to agree that SHI irradiation leads to point defect production in SiC and partially restores crystallinity in a heavily damaged SiC. Epitaxial growth from the amorphous crystalline zone (a-c) is also achieved. This phenomenon has been termed swift heavy ion-beam-induced epitaxial recrystallization (SHIBIEC) and is believed to be due to electronic energy deposition by SHIs and thermal spikes. These previous studies have given less attention to the effect of SHI irradiation on the migration of initially implanted fission products. Only the migration behaviour of Iodine implanted into 6H-SiC at 600 °C has been investigated after SHI irradiation [17]. The results suggested no influence of swift heavy ions on the migration of Iodine in 6H-SiC. In the above mentioned previous studies, the reported SHI irradiations were performed at 33 keV/nm and 20 keV/nm with the maximum SHI irradiation fluences below 10^{14} cm^{-2}.

In this study we report on the effect of 167 MeV Xe^{+26} ion irradiation to fluence of 8.3×10^{14} cm^{-2} on polycrystalline SiC implanted with Kr and Xe.

2. Experimental Method

The starting materials were polycrystalline SiC from Valley Design Corporation. Before implantation, the samples were characterized using scanning electron microscopy (SEM) and electron backscattered diffraction (EBSD). Details of the analyses can be found in [3]. Analysed specimens were composed of mainly columnar crystallites, with diameters of a few micrometers, aligned along the growth direction. Smaller crystals not parallel to the columns were also observed. EBSD analysis indicated that the lattice structure was mainly cubic, but some hexagonal growth modes were also present. The long thin columnar crystals exhibiting numerous planar defects and twinning were found to be frequently occurring. The top surface (where the implantation was done) had clusters of small crystals surrounded by larger crystals, which form the columnar structure.

360 keV Krypton (Kr) and Xenon (Xe) ions were implanted into different polycrystalline SiC wafers up to fluences of 2×10^{16} cm^{-2} and 1×10^{16} cm^{-2} respectively. The implantations were performed a room temperature. Target heating was minimised by keeping the dose rate below 10^{13} cm^{-2}s^{-1} during implantation. Implanted polycrystalline SiC wafers were subsequently irradiated with 167 MeV Xe ions up to fluence 8.3×10^{14} cm^{-2} at room temperature using the IC-100 FLNR JINR cyclotron in Dubna, Russia. Ion beam homogeneity over the samples surfaces was achieved by the use of 2-dimensional beam scanning.

Radiation damage retained after implantations (of Kr and Xe ions into polycrystalline SiC) and after SHI irradiation was investigated by transmission electron microscopy (TEM) and Raman spectrometry. Cross-sectional TEM specimens were prepared using an FEI Helios Nanolab 650 FIB. Thinning of the specimens were performed by successive 30 keV and 5 keV Ga ions. Final polishing was done at 2 keV. TEM specimens were analysed using a JEOL JEM 2100 LAB6 transmission electron microscope operating at 200 kV.

Raman analysis was performed using a HR-800 Raman spectrometer from Jobin-Yvon using a 514.5 nm laser line as excitation source. Collection of the scattered light in the backscattering geometry was made through an Olympus confocal microscope with a 100× objective lens attached.

Depth profiles of the implanted elements before and after swift heavy ion irradiations were obtained by Rutherford backscattering spectrometry (RBS) at room temperature using He^{1+} ions with energy of 1.6 MeV. This was achieved by assuming a SiC density of 3.21 g cm^{-3}. The experimental setup used in this study is discussed in [6].

3. Results and Discussion

Fig. 1 (a) and (b) shows TEM micrographs of Kr implanted SiC and Kr implanted into SiC after SHI irradiation with Xe (167 MeV) at room temperature at a fluence of 8.3×10^{14} cm^{-2} respectively. Kr implantation into SiC at room temperature amorphized the SiC up to a depth of 186 nm. This is in agreement with the published RBS combined with channelling result of Kr (360 KeV) implanted into 6H-SiC at room temperature [11]. SHI irradiation of the Kr implanted SiC caused a reduction of the amorphous layer thickness from 186 to 159 nm. This shrinking of amorphous layer took place from the a-c interface towards the damaged region. Comparing the selected area diffraction (SAD) patterns of the implanted regions before and

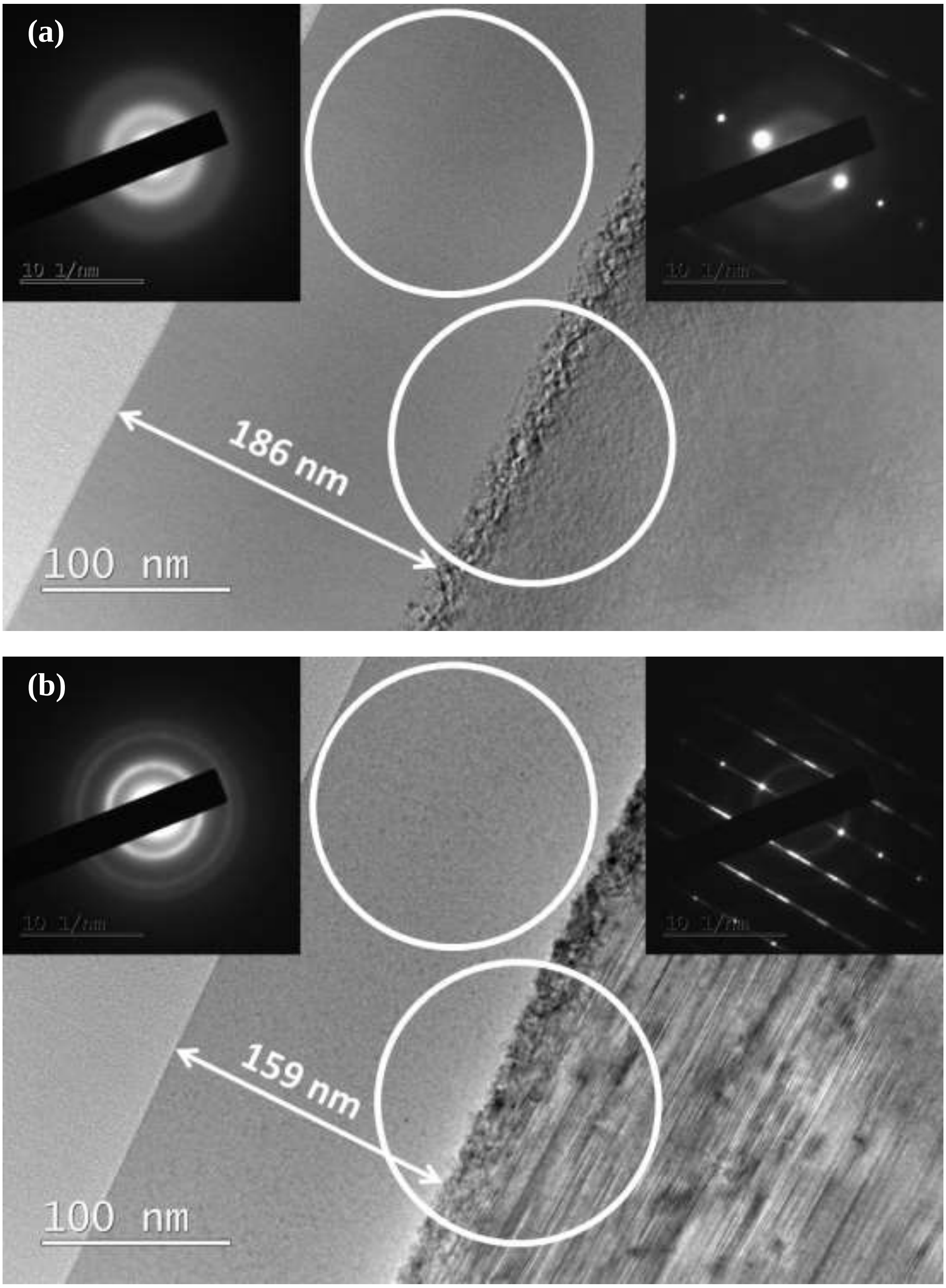

Fig.1. TEM micrograph of polycrystalline SiC implanted with Kr to 2×10^{16} cm^{-2} (a) and subsequently irradiated with Xe (167 MeV) at a fluence of 8.3×10^{14} cm^{-2} (b). The SADs of amorphous and amorphous-crystalline (a-c) interface are also incorporated. The locations where the SADs were taken are indicated by the circles.

after SHI irradiation, the diffuse rings in Fig 1. (a) were replaced by more defined rings after SHI irradiation as seen in Fig1. (b). This suggests some recrystallization and the formation of small randomly oriented crystallites. Looking at the Bright Field (BF) image itself one can notice that after SHI irradiation there is more contrast in the irradiated zone due to the small crystallites. Depending on their orientation with respect the beam they appear at different intensities and thus produce this contrast variation. The other SADs in Fig. 1 (a) and (b) were taken over the a-c interfaces as shown. Each contains only spots for SiC in a single orientation. This means that the crystal structure is continuous from the bulk up to the amorphous region and thus the recrystallization was epitaxial. Similar recrystallization results have been reported [16-23] for both 33 keV/nm and 20 keV/nm electronic energy losses at fluences below 10^{14} cm^{-2}. A very high density of planar defects is also visible in the SHI irradiated specimen and accompanying diffraction pattern. These defects are common in this type of SiC and are not as a consequence of SHI irradiation as the defects were found to be present in various crystallites throughout the poly-crystalline specimen, even beyond the SHI projected range R_p = 13.02 µm (from SRIM). These only produce strong contrast when orientated parallel to the electron beam (like most defects) and therefore they will only be visible for certain crystal orientations since they always lie on their habit plane. The material is polycrystalline and as can be seen from the SADs, the crystals are of different orientation, and therefore the contrast of these defects is much higher in the bottom image. The defects are present in both specimens though. Weak contrast can be observed at the top right corner of Fig. 1 (a) revealing some defects. The defects are not present in the amorphous regions since crystal defects cannot appear if you do not have a crystal.

In addition to the epitaxial growth of the amorphous layer from the a-c interface after SHI irradiation, high resolution TEM micrographs of the amorphous region after SHI irradiation indicated small randomly orientated nanocrystallites as seen in the high resolution TEM

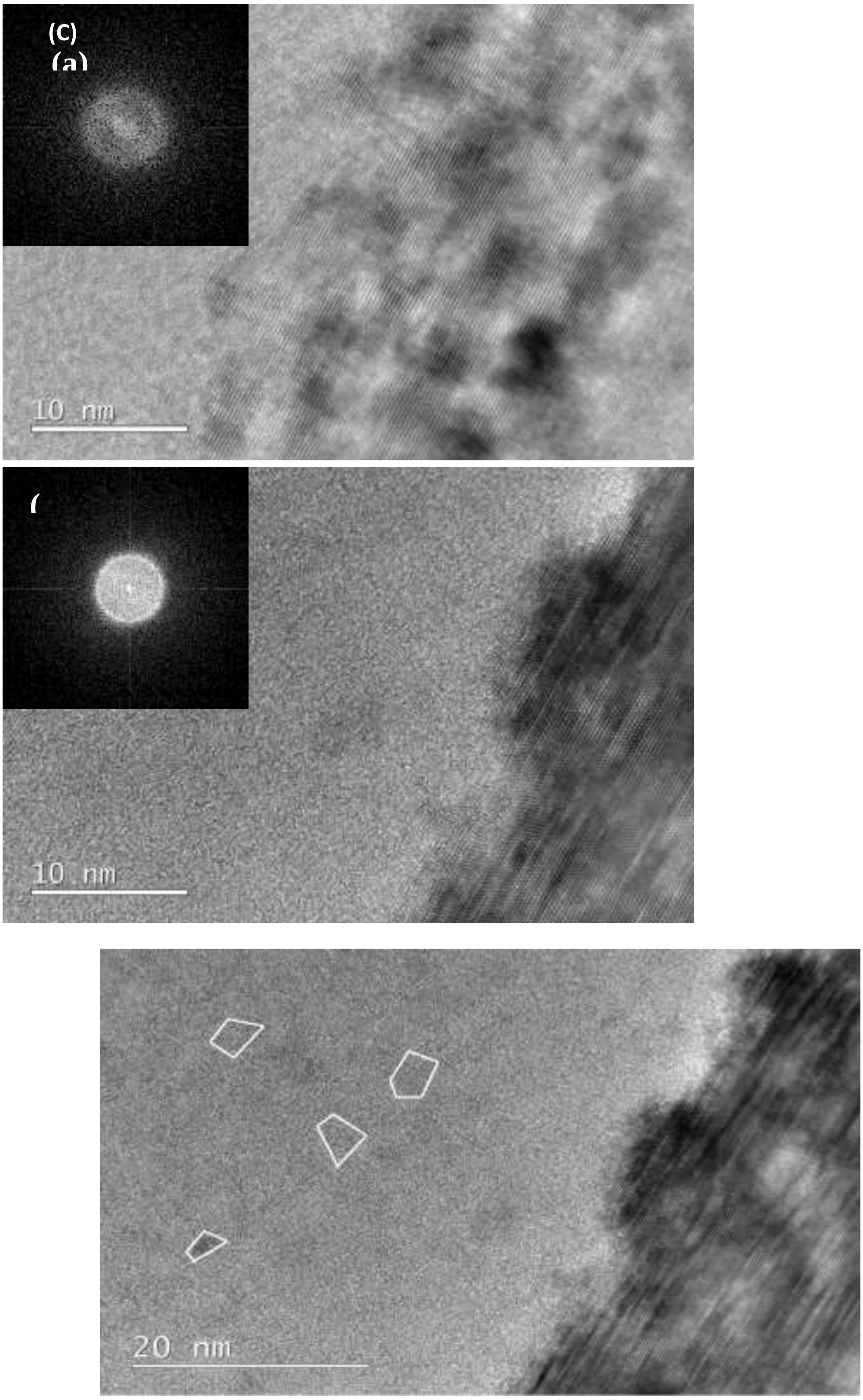

Fig.2. High resolution TEM micrographs of the a-c interface, for as-implanted (a) and after SHI irradiation to a fluence of 8.3×10^{14} cm^{-2} (b), (c) in (c) few nanocrystals are marked. Right and left are the crystalline and the amorphous region respectively. The fast Fourier transforms (FFTs) of amorphous region are included.

micrographs taken across the a-c interface in Fig. 2. The fast Fourier transforms (FTTs) of the amorphous regions before (Fig. 2 (a)) and after SHI irradiation (Fig. 2 (b). are incorporated. The FFT of Fig. 2 (a) appears much more diffuse while for Fig. 2 (b) has a distinct ring around the periphery of the bright region. The latter suggests a higher level of ordering and thus the presence of small crystals randomly orientated. Some nanocrystals are marked in Fig 2 (c.) To our knowledge, no appearance of nanocrystals in SHI irradiated SiC has been previously reported. The lack of observations of nanocrystals formation in amorphous regions after SHI irradiation in previously reported results could be that nanocrystals are only formed at fluences of the order of 10^{14} cm^{-2} i.e. after multiple overlapping of the ion track regions. This might suggest the existence of a fluence threshold in the formation of SiC nanocrystals in the initial amorphous layer after SHI irradiation. More investigations are required to understand the fluence threshold on the formation of the nanocrystals.

Fig. 3 shows TEM micrographs of SiC implanted with Xe at room temperature before (a) and after (b) SHI irradiation with Xe at a fluence of 8.3×10^{14} cm^{-2} respectively. Implantation of Xe resulted in the amorphisation of the SiC to a depth of about 219 nm. The published RBS channelling results of Xe (360 KeV) implanted 6H-SiC at $1\times10^{16}cm^{-2}$ agrees with this observation [12]. SHI irradiation of Xe implanted SiC led to shrinking of the amorphous layer from 219 to 188 nm. Similar to the Kr implanted specimens, the shrinking of the amorphous layer took place from the a-c interface. Also similar to the Kr case, the diffraction patterns in Fig. 3(a) and (b), show epitaxial growth of the amorphous layer after SHI irradiation. The dark spots (some indicated by “arrows”) in the SHI irradiated specimen in Fig. 3 (b) are SiC nanocrystals. Both low energy ion species amorphized SiC and the SHI irradiation conditions were the same.

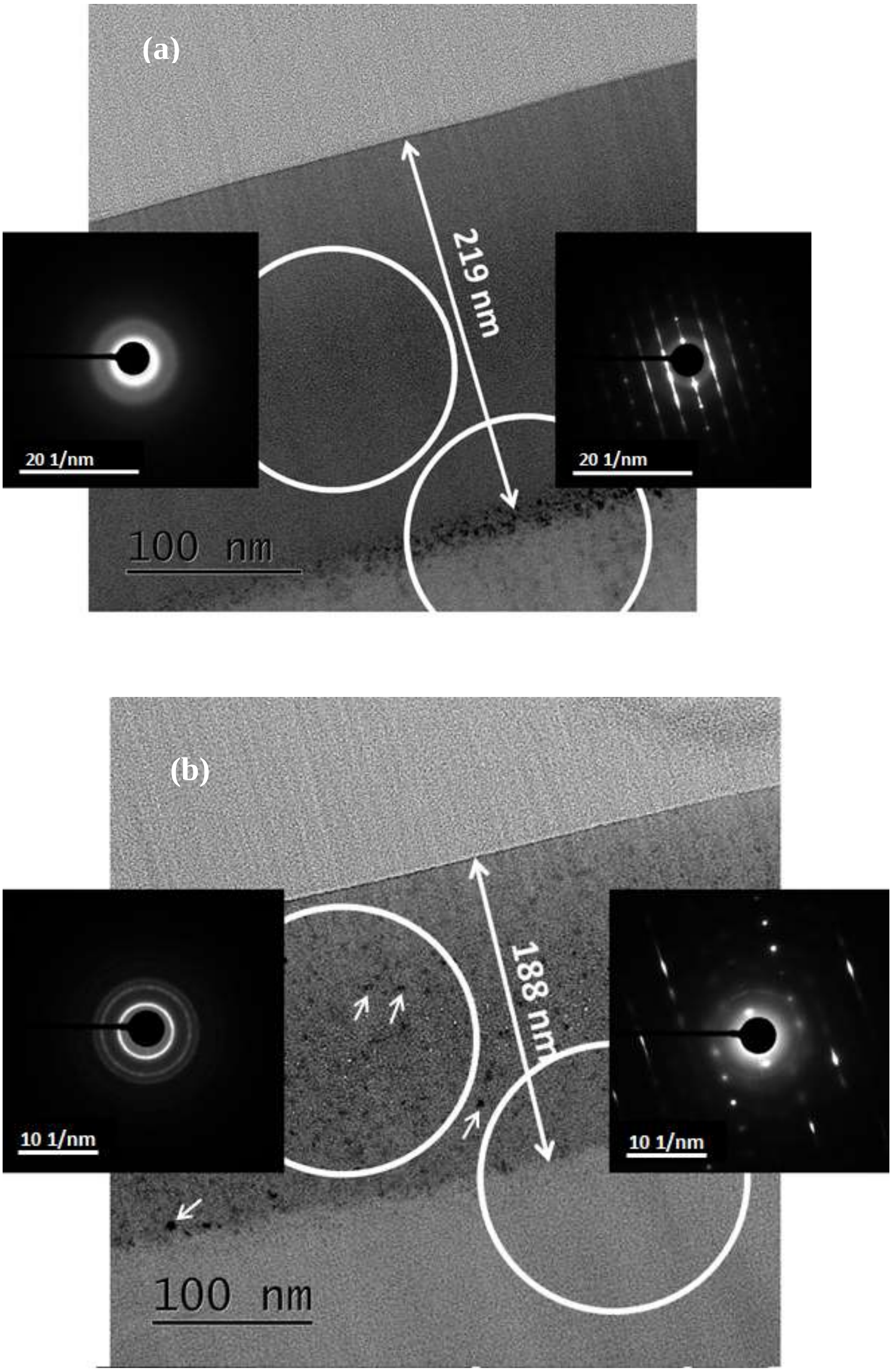

Fig.3. TEM micrograph of polycrystalline SiC implanted with Xe to 1×10^{16} cm^{-2} (a) and subsequently irradiated with Xe (167 MeV) to 8.3×10^{14} cm^{-2} (b). The SADs of amorphous and amorphous-crystalline (a-c) interface are also incorporated. The locations where the SADs were taken are indicated by the circles.

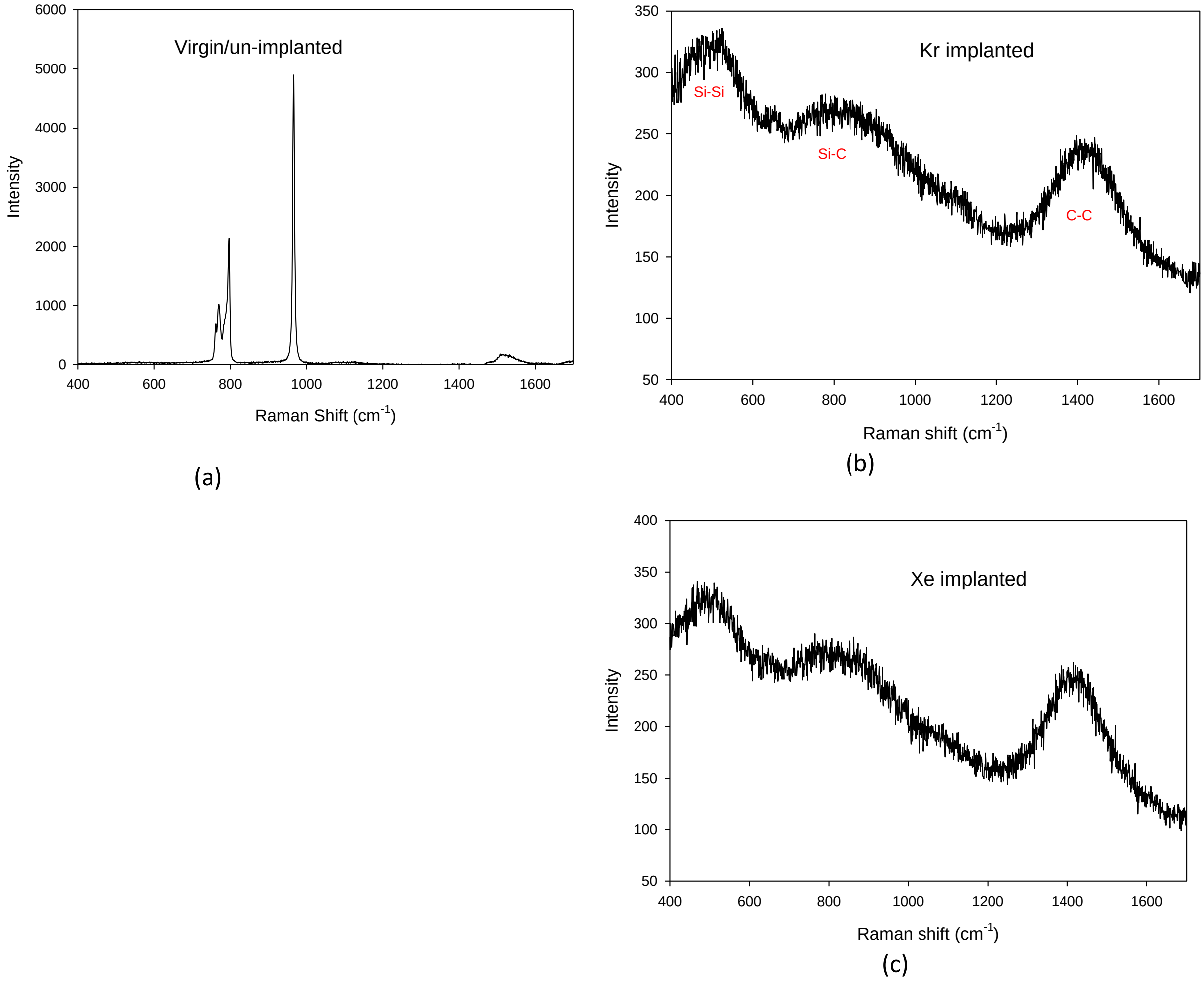

(a)

(b)

(c)

Fig.4. Raman spectra of: (a) virgin polycrystalline SiC, and implanted with 360 keV (b) Kr and (c) Xe ions at room temperature. Virgin polycrystalline (a) showed the Raman characteristics peaks with optical phonon branch above 1500 cm^{-1} [23].

Fig. 4 shows the as-implanted Raman spectra of 360 keV Kr and Xe implanted specimens compared to the un-implanted Raman spectrum. These implantations amorphized the implanted region of the SiC. This is deduced from the disappearance of polycrystalline Raman peaks and the appearance of both Si-Si (around 490 cm^{-1}) and C-C (around 1410 cm^{-1}) Raman peaks. The Raman spectra of the virgin and as-implanted samples agree with the results reported in [24, 25].

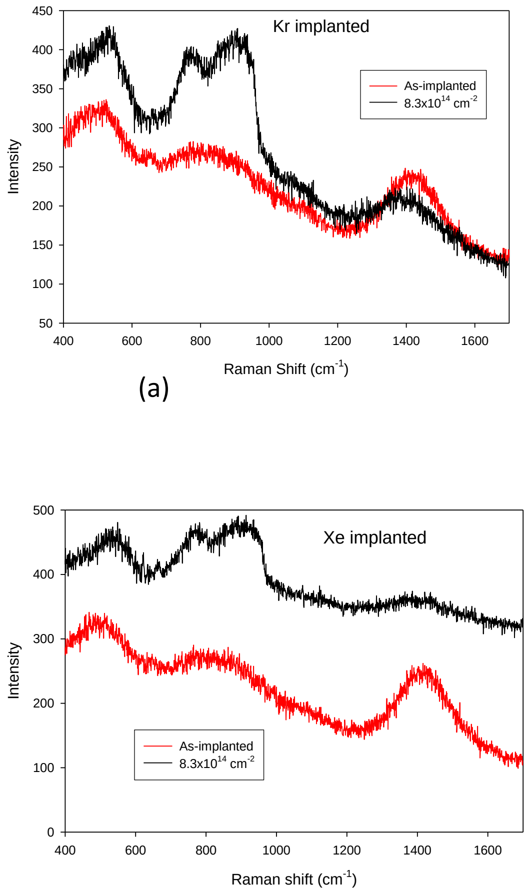

(a)

(b)

Fig.5. Raman spectra of polycrystalline SiC implanted with 360 keV Kr (a) and Xe (b) ions at room temperature compared to polycrystalline SiC (initially implanted with Kr and Xe) and irradiated by 167 MeV Xe ions at room temperature to the fluences indicated in the figures. The Raman peak around 650 cm^{-1} might be noise due to cosmic rays.

The Raman spectra of the SHI irradiated specimens are compared to the spectra of the as-implanted (low energy ions) specimens in Fig. 5. The Si-Si (at about 490 cm^{-1} cm^{-1}) and C-C (at about 1410 cm^{-1}) Raman peaks indicate that the amorphous regions still exist within the as-implanted layer. SHI irradiation at this fluence caused some recrystallization as indicated by the reappearance of broad (in contrast to the characteristic sharp peaks) SiC peaks around 775 and 895 cm^{-1}. These broad Raman peaks at 775 and 895 cm^{-1} roughly correspond to the sharp peaks of virgin SiC shown in Fig. 4 (a). The fact that these two peaks are now broader and partially merged indicates that the SiC was no longer fully amorphized but now partially crystallised, i.e. still damaged [26].

There are two possible reasons for this evidence of crystallinity in SiC samples. These could be due to either sampling of the crystal below the amorphous regions in the as-implanted specimen, or to some crystalline order in the amorphous region. It is unlikely that partial reappearance of the characteristic SiC Raman peaks in the SHI bombarded samples was due to penetration of the excitation laser light through the amorphous layer into the polycrystalline bulk. Our argument is based on the thicknesses of the amorphous layers before and after SHI bombardment. The above TEM results (cf. Figure 3) showed that the thickness of the Xe implanted samples after SHI irradiation reduced to 188 nm. This is essentially the same thickness of the Kr implanted samples before SHI bombardment, viz. 186 nm. In the latter case the Raman spectrum was that of amorphous SiC.

Therefore, the partial reappearance of the characteristic SiC Raman peaks after SHI irradiation can only be due to the growth of small SHI-induced crystallites in the amorphous layers. Based on the solid state epitaxial growth model [27], these crystals probably started from small seed crystals within the amorphous layers. The (partial) reappearance of SiC Raman peaks is also consistent with the TEM observation of nanocrystals formation (see Figures 2 and 3). The diffraction patterns of these regions show diffuse rings remaining in the as-implanted specimen. This implies that some degree of short range ordering is still present while the diffuseness of the rings suggests an interatomic spacing that is a distribution around some average value rather than a consistent value that characterizes a crystal. This is to be expected since the original material was crystalline. Therefore, even though for most considerations (and all practical applications) the material can be considered amorphous, there is some degree of remaining short range correlation. After SHI irradiation, ordering becomes more long range as is evident from the rings in the SAD becoming more refined (sharper) and broad peaks start appearing around 775 and 893 cm^{-1}.

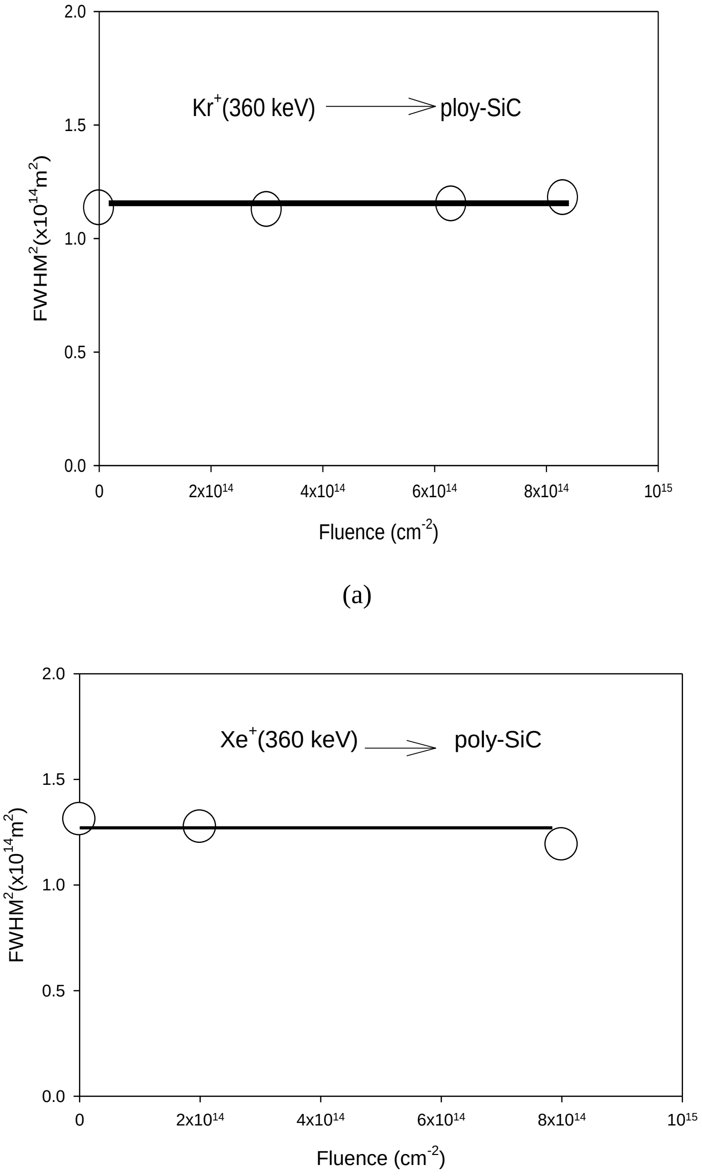

(a)

(b)

Fig. 6*:* Squares of the full width at half maximum, i.e. (FWHM)^2, of the profiles of the implanted Kr(a) and Xe (b) (taken from the RBS data not shown) as a function of SHI irradiation fluence. The statistical error (standard deviation) of the data is within the symbols used in the graphs.

In order to determine whether diffusion took place during swift heavy ion irradiation, depth profiles obtained from RBS were fitted to an Edgeworth function. The Edgeworth function is a modified Gaussian function which also has the next two higher moments (kurtosis and skewness) [28].

The plots of FWHM squared as function of irradiation fluence are depicted in Fig. 6. The horizontal straight lines given in the two graphs are only there to guide the eye. They show that the data is either fluence-independent or that there is only a very slight dependence on the fluence. More data points are needed to make any meaningful conclusion. The statistical error (standard deviation) of the data is within the symbols used in the graphs. From these results it is quite clear that the depth profiles did not broaden after swift heavy ion irradiation indicating no detectable diffusion for all the implanted species. Similar results indicating the absence of diffusion of I implanted in SiC after swift heavy ion irradiation have been reported by Audren *et al.* [17].

4. Conclusions

Individual implantation of 360 KeV Kr (up to a fluence of 2×10^{16}cm^{-2}) and Xe (up to a fluence of 1×10^{16}cm^{-2}) ions in polycrystalline SiC at room temperature completely amorphized the matrix to a depth of 186 and 219 nm respectively. SHI irradiation at room temperature up to 8.3×10^{14} cm^{-2} of the implanted specimens resulted in the shrinking of the amorphous region from the amorphous-crystalline (a-c) interface for both samples. This was due to epitaxial growth of the amorphous layer from the a-c interface after SHI irradiations. High resolution TEM analyses together with fast Fourier transforms indicated that the epitaxial growth from the a-c interface was accompanied by the formation of randomly orientated nanocrystals in the former amorphous region. The formation of the nanocrystals has not been reported before by SHI irradiation experiments performed at fluences below 10^{14} cm^{-2}. This might suggest a SHI fluence threshold for the formation of these nanocrystals.

This fluence threshold is probably related to the onset of swift heavy ion tracts overlapping with each other, with a subsequent higher energy deposition in the implanted area.

Raman investigations using a visible light (514.4 nm) excitation laser confirmed the existence of an amorphous layer on the SiC after low energy (i.e. 360 keV) implantation of Kr^+ and Xe^+ ions. The Raman spectra after SHI irradiation showed the reappearance of the characteristic SiC Raman peaks albeit still very broad, small and less distinct. This could be interpreted as either the formation of small SiC crystallites in the amorphous layer or a thinner amorphous layer allowing the penetration of the light through the amorphous layer to the polycrystalline substrate. It was argued that the latter was unlikely based on the thicknesses of the layers before and after SHI bombardment. The TEM results confirmed the growth of small SiC crystals in the amorphous layers after SHI irradiation.

The RBS spectra of the implanted Kr and of Xe profiles showed no broadening of the peaks after SHI irradiation. This means that no diffusion of the implanted species was detected after SHI irradiation.

To get more insight in the formation of nanocrystals after SHI irradiation, more investigations are required to determine the exact threshold.

5. Acknowledgements

Thanks are due to Prof. E. Friedland for useful discussions, Dr. Linda Prinsloo for the assistance with Raman and National Research Foundation (NRF) of South Africa for funding.

6. References

1. http://www.world-nuclear.org/info/Nuclear-Fuel-Cycle/Power-Reactors/Generation-IV-Nuclear-Reactors/; 31January 2015.
2. J.B. Malherbe, E. Friedland and N.G. van der Berg,"Ion beam analysis of materials in the PBMR reactor" Nucl. Instr. Meth. B, **266**[8] 1373-1377 (2008).
3. E. Friedland, J.B. Malherbe, N.G. van der Berg, T. Hlatshwayo, A.J. Botha, E. Wendler and W. Wesch,"Study of Silver Diffusion in Silicon Carbide" J. Nucl. Mater., **389** [2] 326-331 (2009).
4. E. Friedland, N.G. van der Berg, J.B. Malherbe, J.J. Hancke, J.R.N. Barry, E. Wendler and W. Wesch, "Investigation of silver and iodine transport through silicon carbide layers prepared for nuclear fuel element cladding" J. Nucl. Mater., **410** [1-3] 24-31 (2011).
5. T.T. Hlatshwayo, J.B. Malherbe, N.G. van der Berg, L.C. Prinsloo, A.J. Botha, E. Wendler and W. Wesch,"Annealing of silver implanted 6H-SiC and the diffusion of the silver" Nucl. Instr. Meth. B, **274** 120-125 (2012).
6. T.T. Hlatshwayo, J.B. Malherbe, N.G. van der Berg, A.J. Botha and P. Chakraborty,"Effect of thermal annealing and neutron irradiation in 6H-SiC implanted with silver at 350 °C and 600 °C " Nucl. Instr. Meth. B, **273** 61-64(2012).
7. J. B. Malherbe, "Diffusion of fission products and radiation damage in SiC" J. Phys. D: Appl. Phys., **46** 473001 27 pp (2013).
8. T.T. Hlatshwayo, N.G. van der Berg, M. Msimanga, J.B. Malherbe and R.J. Kuhudzai,"Iodine assisted retainment of implanted silver in 6H-SiC at high temperatures" Nucl. Instr. Meth. B, **334** 101-105(2014).
9. M.B. Mukhawana, C.C. Theron, J.B. Malherbe, N.G. van der Berg, A.J. Botha, W. Grote, E. Wendler, W. Wesch and P. Chakraborty, " Behavior of iodine implanted in

highly oriented pyrolytic graphite (HOPG) after heat treatment" Nucl. Instr. Meth. B, **273** 65-67 (2012).

10. D.F. Langa, N.G. van der Berg, E. Friedland, J.B. Malherbe, A.J. Botha, P. Chakraborty, E. Wendler and W. Wesch, "Heat treatment of glassy carbon implanted with cesium at room and high temperatures" Nucl. Instr. Meth. B, **273** 68-71 (2012).
11. E. Friedland, T.T. Hlatshwayo, N.G. van der Berg and M.C. Mabena,"Influence of radiation damage on krypton diffusion in silicon carbide" Nucl. Instr. Meth. B, **354** 42–46 (2015).
12. E. Friedland, K. Gartner, T.T. Hlatshwayo, N.G. van der Berg and T.T. Thabethe, "Influence of radiation damage on xenon diffusion in silicon carbide " Nucl. Instr. Meth. B, **332** 415-420 (2014).
13. R.L. Fleischer, P.B. Price, R.M. Walker, Nuclear Tracks in solids, University of California Press, Berkeley, CA, 1975.
14. V.A. Skuratov, N. Dinu, I.V. Antonova and V. I. Obodnikov, "Hundred MeV heavy ion irradiation on boron diffusion in Si" Vaccum, **63**[4] 571-575 (2001).
15. E.P. Neustroev, I.V. Antonova, V.I. Obodnikov, V.P. Popov, V.A. Skuratov, S.A. Smagulova and A.Yu. Didyk, "Impact of high energy ion implantation on dopant distribution in silicon", Nucl. Instr. Meth. B, **146**[1-4] 323-328 (1998).
16. A. Benyagoub, A. Audren and F. Garrido, "Athermal crystallization induced by electronic excitations in ion-irradiated silicon carbide", Appl. Phys. Lett, **89** 241914 3pp (2006)
17. A. Benyagoub, "Irradiation effects induced in silicon carbide by low and high energy ions" Nucl. Instr. Meth. B, **266**[12-13]2766-2771 (2008).
18. A. Audren , A. Benyagoub, L Thome and F. Garrido, "Ion implantion of iodine into silicon carbide: Influence of temperature on the produced damage and on the diffusion behaviour" Nucl. Instr. Meth. B, **266** [12-13] 2810-2813 (2008).

19. A. Benyagoub and A. Audren, “Study of the damage produced in silicon carbide by high energy heavy ions” Nucl. Instr. Meth. B, **267**[8-9]1255-1258(2009).

20. V.A. Skuratov, J. O’Connell, A.S. Sohatsky and J. Neethling, “TEM study of damage recovery in SiC by swift Xe ion irradiation” Nucl. Instr. Meth. B, **327** 89-92 (2014).

21. J. H. O’Connell, V. A. Skuratov, A. S. Sohatsky and J .H. Neethling, “1.2 MeV/amu Xe ion induced damage recovery in SiC” Nucl. Instr. Meth. B, **326** 337-340(2014).

22. A. Debelle, M. Backman, L. Thomé, K. Nordlund, F. Djurabekova, W. J. Weber, I. Monnet, O. H. Pakarinen, F. Garrido and F. Paumier, “Swift heavy ion induced recrystallization in cubic silicon carbide: New insights from the designed experiments and MD simulations” Nucl. Instr. Meth. B, **326** 326-331(2014).

23. S. Sorieul, X. Kerbiriou, J-M Costantini, L. Gosmain, G. Calas and C. Trautmann, “Optical spectroscopy study of damage induced in 4H-SiC by swift heavy ion irradiation” J. Phys. Condens. Matter, **24** 125801 7pp (2012).

24. J. Camassel, S. Blanque, N. Mestres and P. Godignon and J. Pascual , “Comparative evaluation of implantation damage produced by N and P ions in 6H-SiC”, Phys. Stat. Sol. (c), **3** 875-880 (2003).

25. S. Sorieul, J-M. Costantini, L. Gosmain, L. Thomé and J-J Grob, “Raman spectroscopy study on heavy-ion-irradiated α-SiC ” J.Phys. Condens. Matter, **18** 5235-5251 (2006).

26. L. Thomé , G. Velisa, A. Debelle, S. Miro , F. Garrido , P. Trocellier , Y. Serruys, Nucl. Instr. Meth. B, **326** , 219-222 (2014).

27. F.C. Frank and J.H. van der Merwe, “One dimensional dislocations”, Proc. Royal Soc **198**, 205 (1949).

28. T.T. Hlatshwayo, “Diffusion of silver in 6H-SiC “, PhD thesis, University of Pretoria, (2010).